Peer-reviewed version available at *Molecules* **2017**, *22*, 1047; doi:10.3390/molecules22071047

The Investigation of Electrochemistry Behaviors of Tyrosinase Based on Directly Electrodeposited Graphene on Choline–Gold Nanoparticals

Yaping He[a,*], Xiaohui Yang[a], Quan Han[a] and Jianbin Zheng[b,*]

[a] *School of Chemical Engineering, Xi'an University, Xi'an, Shaanxi 710065, China*

[b] *Institute of Analytical Science/Shaanxi Provincial Key Laboratory of Electroanalytical Chemistry, Northwest University, Xi'an, Shaanxi 710069, China*

Abstract

A novel catechol (CA) biosensor was developed by the immobilization of tyrosinase (Tyr) onto *in situ* electrochemical reduction graphene (EGR) on choline functionalized gold nanoparticals (AuNPs–Ch) film. The results of UV–visible spectra indicated that Tyr retained its original structure in the film. And electrochemical investigation of the biosensor showed a pair of well–defined, quasi–reversible redox peaks with E_{pa}= –0.0744V and E_{pc}= –0.114 V (*vs*. SCE) in 0.1 M, pH 7.0 sodium phosphate buffered saline at the scan rate of 100 mV/s. The transfer rate constant k_s was 0.66 s^{-1}. The Tyr–EGR/AuNPs–Ch showed a good electrochemical catalytic response for the reduction of CA, with the linear range from 0.2 to 270 μM and a detection limit of 0.1 μM (S/N= 3). The apparent Michaelis–Menten constant was estimated to be 109 μM.

Keywords: electrochemistry; tyrosinase; graphene; Choline–gold nanoparticals; catechol

* Corresponding author. Tel: +86 29 88258553. Fax: +86 29 88258553.

E-mail: hejin04c@126.com

* Corresponding author. Tel: +86 29 88373025. Fax: +86 29 88303448.

E-mail: zhengjb@nwu.edu.cn

Peer-reviewed version available at Molecules 2017, 22, 1047; doi:10.3390/molecules22071047

1. Introduction

Phenolic compounds are a very important and widespread class of substances[1]. However, they are toxic, and injure mammals, fishes and other aquatic organisms[2]. They are on the priority pollutants list of European Community and the environmental Protection Agency of United States because of their toxicity and persistency in environment[3]. The determination of phenols is of paramount importance in both environmental analysis, medical and food quality characterization. The commonly used analytical methods for the determination of phenols are spectrophotome and chromatography [4]. These techniques evertheless have a number of disadvantages such as expensive, time–consuming and difficult to apply *in situ* [3], which limit their applications primarily to laboratory settings and prohibit their use for rapid analyses under field conditions. Many efforts have been devoted to develop a simple and effective analytical method for the determination of phenols. Electrochemical biosensor has been considered as the best choice for *in situ* monitoring of phenolic compounds by virtue of its high sensitivity, simple instrumentation, low production cost and promising response speed [5], However, determination of phenols through the direct electrochemical is suffered from a number of drawbacks due to the high overvoltage, a high anodic potential needs to be applied, which open up the detection system for interfering reactions [6]. And, the high applied voltage is also followed by an increase of background current and noise level. Furthermore, direct electrochemical oxidation of phenols is coupled with fouling reactions [7]. Electrochemical biosensors based on enzymes are suitable for a highly selective, sensitive, and rapid analysis of phenols in various biological species *in vivo* and *in vitro* [8]. And, enzyme–based amperometric biosensors for the determination of phenols have been experimentally demonstrated as an efficient route to solve the obstacles above mentioned.

Tyrosinase (Tyr), known as polyphenol oxidase, is a copper monooxygenase that catalyzes oxidation of phenolic compounds to their corresponding o–quinines [9] that can be electrochemically reduced to allow convenient low–potential detection of phenolic analytes [10]. It belongs to Type 3 copper proteins family, a single dicopper enter being responsible for the oxidation of phenolic substrates with oxygen as co–substrate[11]. Electrochemical biosensors based on Tyr are simple and convenient tools for phenol assays due to their high sensitivity, effectiveness and simplicity [12]. Many nanomaterials, such as carbon–coated nickel nanoparticles[13], polyaniline (PANI) [14], hydroxyapatite [15], Fe_3O_4 nanoparticles [4], ZnO nanorod microarrays [16] and sonogel–carbon [17] have been used to construct Tyr biosensor for the detection of catechol (CA). It shows advantages of good reliability, fast response, inexpensive instrument, low energy consumption, simple operation, time saving and high sensitivity [18]. Unfortunately, redox peaks, corresponding to the T3 site, could not be seen on cyclic vohammetry (CV) scans, performed under anaerobic conditions [19]. The direct electrochemistry of Tyr

Peer-reviewed version available at Molecules 2017, 22, 1047; doi:10.3390/molecules22071047

is commonly hard to be observed. There are only a few literatures that described the direct electrochemistry of Tyr based on Woodward's Reagent K[20], single–walled carbon nanotubes (SWCNTs) [21, 11], gold nanoparticles (AuNPs)[22] and Nickel oxide nanoparticles (NiONPs)[23].

Carbon can act as a primary electron donor to native electroactive site of enzymes [17]. As the "rising star" in the carbon nanomaterial family, graphene (GR) have attracted more and more attentions in the preparation of sensors and biosensors [24–26] due to their large surface area, extraordinary electronic transport property, high electrocatalytic activity, good mechanical strength, high thermal conductivity and high mobility of charge carriers [27–29]. Our group has successfully achieved the direct chemistry of hemoglobin and glucose oxidase with GR–based materials [30, 31]. Electrochemical methods are one of the most promising environment friendly (without using any toxic solvents) methods to obtain GR via graphene oxide (GO) and it is simple, fast, cost–effective and it is more suitable for preparing less defective graphene sheet [32–34]. Sensors for the determination of ascorbic acid, hydrazine hydrate and glucose have been fabricated by us through the direct electrodepositing GR on the surface of the bare electrode [35–37]. GR functionalized with biocompatible materials [38], makes it water–soluble and biocompatible, which can act as a novel material promising for biological applications [39]. Biocompatible GR as a sensor platform not only present an abundant domain for bimolecular binding but also play a role of fast electron–transfer kinetics and further signal amplification in electrochemical detection [40].

AuNPs possess distinct physical and chemical attributes that make them excellent scaffolds for the fabrication of novel chemical and biological sensors [41]. Electrochemical studies have revealed that AuNPs can enhance electrode conductivity, facilitating the electron transfer and improving the detection limit for biomolecules [42]. Self–assembled monolayers of AuNPs attached to alkane or aromaticthiols terminated with functional groups –SH or $–NH_2$ is useful for the preparation of AuNP–modified electrodes. AuNPs have been successfully used for bioanalytical applications because of low cytotoxicity, high affinity with molecules of thiol/amine containing groups, and offering suitable platforms for surface immobilization of a wide range of enzymes and biomolecules [43]. Undoubtedly, the merits of GR and AuNPs contributed to the high sensitivity of biosensors [31]. graphene–AuNPs composites have been well prepared and used as the electro-catalysts for biosensing glucose, oxygen, and uric acid[44].

Under the condition of electrochemical oxidation, the hydroxyl of choline (Ch) reacted with the cation radicals on the surface of glassy carbon electrode (GCE) to fabricate –C–O–C– bond, which was covalently grafted on the surface of GCE [45]. The quaternary ammonium $–N^+(CH_3)_3$ functional groups

Peer-reviewed version available at Molecules 2017, 22, 1047; doi:10.3390/molecules22071047

of the choline modified layer were with positive charge, which may interact with the negatively charged nanobiocomposite film such as AuNPs [46]. The choline layer could not only fix Au colloids but also promote the direct electron transfer of proteins [45].

As mentioned above, a biocompatible GR film can easily fabricate with Ch–AuNPs as linker to bare GCE, and acted as the attachment sites for the directly electrodeposion of graphene (EGR). The aim of the present work is to *in situ* fabricate EGR–AuNPs–Ch biocompatible film and immobilize Tyr onto it. The electrochemical behavior of Tyr and its electrocatalysis towards catechol (CA) in the proposed biosensor is further investigated.

2. Experimental

2.1. Materials and apparatus

Tyr from Mushroom (3610 Umg^{-1}), Nafion (5% m/v in methanol) and Chloroauricacid tetrahydrate ($HAuCl_4 \cdot 4H_2O$) were purchased from Sigma. Choline chloride [$HOC_2H_4N(CH_3)_3Cl$] (ChCl) was purchased from Sinopharm Chemical Reagent Co. Ltd (Shanghai, China), Ethylene glycol (EG) was got from Tianjin TianLi Chemical Reagent Ltd (Tianjin, China). High purity graphite powder was purchased from Shanghai Carbon Plant (Shanghai, China). High purity graphite powder was purchased from Shanghai Carbon Plant (Shanghai, China). CA was purchased from Tianjin Kemiou Chemical Reagent Co., Ltd (Tianjin, China). All other chemicals were of analytical reagent grade and doubly distilled water was used in all the experiments. A 0.1 M pH 7.0 sodium phosphate buffered saline (PBS) was used in all electrochemical studies.

All electrochemical experiments were carried out on a CHI 660D electrochemical workstation (Shanghai CH Instrument Co. Ltd., China) using a three electrode system. The working electrode was GCE or modified GCE. GCE of 3–mm diameter, before use, was first polished to a mirror–like surface with 1.0, 0.3 and 0.05 μm Al_2O_3 slurry on a polish cloth, and rinsed with double–distilled water, then sonicate treated in ethanol and double–distilled water for 5 min, respectively. Then, the electrode was allowed to dry under nitrogen. A saturated calomel electrode (SCE) and a platinum electrode were served as reference and counter electrodes, respectively. UV–vis spectra were obtained on a UV–vis spectrophotometer attached to ELx800 Absorbance Microplate Reader (BioTek, USA). Herein, ITO (Hebei Lingxian Gaoke Co. Ltd.) was used as the substrate for the investigation of the morphology. Before use, it was cleaned by sonicate treatment sequentially for 20 min in acetone, 10% KOH in ethanol and distilled water. Scanning electron microscopic (SEM) measurements were carried out on

JSM–6700F (Japan Electron Company, Japan) at 15 kV. All the electrochemical experiments were conducted at room temperature (25±2 °C).

2.2. Preparation and modification of the Nafion/Tyr/EGR–AuNPs–Ch/GCE

EG and ChCl (2:1) were gentle heated by continuous stirring until a homogeneous solution formed. 500 μL of $HAuCl_4$ solution (w/w, 1%) was added into 50 mL of the above solution. Then, 5 mL of sodium borohydride solution (w/w, 1%) was slowly added, while stirring vigorously. Kept the wine red solution stirring at 50 °C for another 30 mins. Then, allowed it to cool down and AuNPs–Ch was prepared and stored at 4 °C for use.

GO was synthesized from graphite powder by a modified Hummers method [47]. The fabrication process of the Nafion/Tyr/EGR–AuNPs–Ch/GCE was as following: 10 μL of AuNPs–Ch homogeneous solution was casted onto the surface of the GCE by using a syringe to prepare AuNPs–Ch/GCE. The modified electrode dried at room temperature later. The preparation of electrolyte solution: 1 mg/mL GO was dispersed in 1/15 M, pH 9.18 PBS, and ultrasonication–mixed for several minutes to form a homogeneous solution. Prior to experiments, the solution was deoxygenated with high purity nitrogen gas. The electrochemical deposition of EGR on the AuNPs–Ch/GCE was performed in the above eletrolyte solution from –1.5 to 0.5V for 10 circles at the scan rate of 10 mV/s. The treated substrate electrode was washed with distilled water. 10 μL of Tyr (5 mg/mL in pH 7.0 PBS) was cast onto the electrode surface by using a syringe to prepare Tyr/EGR–AuNPs–Ch/GCE. Then, 3 μL of 0.5 wt% Nafion was dropped on it. Dried in room temperature later, the sensor was stored at 4 °C when not in use.

3. Results and discussion

3.1. Fabrication and characterization of the Nafion/Tyr/EGR –AuNPs–Ch/GCE

As shown Scheme 1A, electrostatic assembly of positively charged $–N^+(CH_3)_3$ polar head group of Ch with $AuCl_4^–$. The surface modification of gold nanospheres with choline was prepared by the reduction process. And the superficial choline has hydroxy groups, which could be covalently bound to the edge plane sites of the carbon surface through the oxygen atom [48]. Thus, –C–O–C– bond was formed, which made the efficiently immobilization of AuNPs–Ch onto the bare GCE. AuNPs–Ch was fixed on the GCE, as shown in Scheme 1B. The presence of oxygen containing groups [29] handle GO

Preprints (www.preprints.org) | NOT PEER-REVIEWED | Posted: 28 April 2017 doi:10.20944/preprints201704.0188.v1

Peer-reviewed version available at Molecules 2017, 22, 1047; doi:10.3390/molecules22071047

exists as a planar sheet that can be inlay into AuNPs–Ch to form large–scale two–dimensional arrays. The further *in situ* electrochemical synthesized GR nanosheets enhanced the interaction with AuNPs–Ch on the electrode surface by the π–π attraction, which can form a stable EGR–AuNPs–Ch. The high surface area of GR was helpful for immobilizing more proteins or enzymes and the nanocomposite film could provide microenvironment for proteins or enzymes to retain its native structure and activity, and to achieve reversible direct electron transfer reaction at the electrode surface [49]. Tyr anchored onto EGR and attached firmly. The addition of Nafion as an immobilization matrix to entrap enzymes and proteins effectively prevented the leakage of Tyr at the outermost.

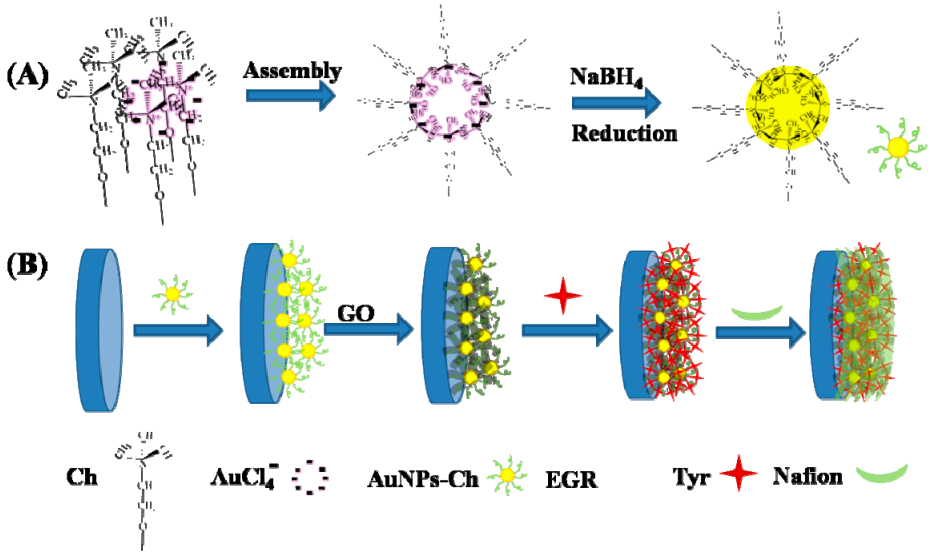

Scheme 1. The fabricate strategy of AuNPs–Ch (A); Schematics of the fabrication process of the Nafion/Tyr/EGR–AuNPs–Ch/GCE (B).

As shown in Fig. 1A, with the electrochemical process from –1.5 to 0.5 V for 10 circles at the scan rate of 10 mV/s, the AuNPs–Ch nanospheres of diameters 70 to 150 nm were inhomogeneous scattered (as shown in Fig. 1B). However, EGR–AuNPs–Ch showed a uniform film with evenly dispersed nanospheres (Fig. 1C). The shrink of AuNPs–Ch of diameters 50 to 120 nm (as shown in Fig. 1D), confirm our fabrication strategy of the EGR–AuNPs–Ch. EGR intercalated the structure of AuNPs–Ch, which restrainted the GR layer overlap and AuNPs agglomerate, creating a favourable "building" for Tyr existence.

UV–visible soret absorption band of Tyr may provide the information on the conformational integrity of the protein and the possible denaturation or the conformational change of active centres region. At the wavelength range from 200 to 350 nm, AuNPs–Ch (Fig 2 curve a) and EGR–AuNPs–Ch had no Soret band, indicating there is no interference of Tyr. Tyr dissolved in PBS had the Soret band at 279.8 nm (Fig 2 curve d), while the Soret band of the Tyr/EGR–AuNPs–Ch was appeared at 280.3 nm

Preprints (www.preprints.org) | NOT PEER-REVIEWED | Posted: 28 April 2017 doi:10.20944/preprints201704.0188.v1

Peer-reviewed version available at Molecules 2017, 22, 1047; doi:10.3390/molecules22071047

(Fig 2 curve d). The difference of Tyr and the Tyr/EGR–AuNPs–Ch was less than 1 nm, indicating that Tyr in the Tyr/EGR–AuNPs–Ch had the microenvironment similar to the native state of Tyr in PBS.

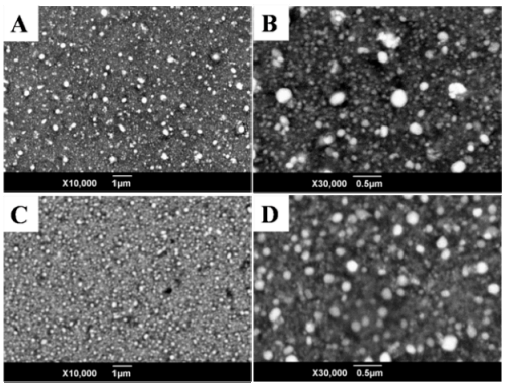

Fig. 1 SEM imagines of E–AuNPs–Ch low magnification(A) and high magnification (B); SEM imagines of EGR–AuNPs–Ch low magnification (C) and high magnification (D).

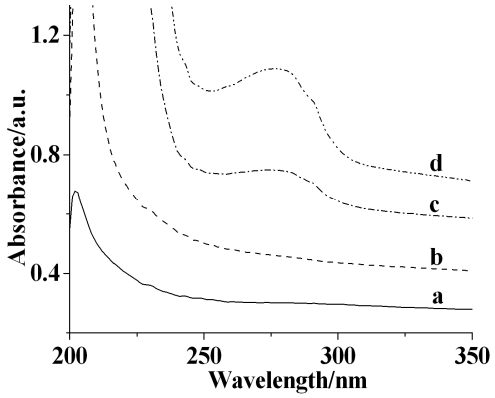

Fig. 2. UV–vis absorption spectra of AuNPs–Ch in PBS (a), EGR–AuNPs–Ch in PBS (b) in the solution of the Tyr/EGR–AuNPs–Ch mixture (c) and 0.3 mg/mL Tyr in PBS (d), and. The path length: 0.05 cm.

Electrochemical impedance spectroscopy (EIS) is an effective method for probing the features of surface modified electrode and can provide information on the impedance changes accompanying the stepwise electrode modification process. As shown in Fig.3B, the semicircle of the AuNPs–Ch/GCE (curve b′) and the EGR–AuNPs–Ch/GCE (curve d′) were obviously smaller than that of the bare GCE (curve a′). The addition of Tyr blocked the electron transfer on the surface of GCE, resulted the increase of the impedance (curve c′), which was in good agreement with the results of CVs.

3.2. Direct electrochemistry of Tyr at the Nafion/Tyr/EGR–AuNPs–Ch/GCE

The direct electrochemisTyr of Tyr at the Nafion/Tyr/EGR–AuNPs–Ch/GCE was studied by cyclic voltammetry (CV). Cyclic voltammograms (CVs) of Tyr with different scan rates were shown in Fig. 4. The Nafion/Tyr/EGR–AuNPs–Ch/GCE showed a pair of well–defined, quasi–reversible redox peaks

Preprints (www.preprints.org) | NOT PEER-REVIEWED | Posted: 28 April 2017 doi:10.20944/preprints201704.0188.v1

Peer-reviewed version available at Molecules 2017, 22, 1047; doi:10.3390/molecules22071047

with E_{pa}= –0.0744V and E_{pc}= –0.114 V (*vs*. SCE) in PBS (0.1 M, pH 7.0) with the formal potential $E^{0\prime}$= –0.0942 V. The value of $E^{0\prime}$ corresponded with the active sites of Tyr from different sources were varied from 120 to 600 mV versus NHE [50]. The peak–to–peak separation ΔE_p was 40 mV and about 1 ratio of cathodic to anodic current intensity at the scan rate of 0.1 V/s. The redox process of Tyr at the Nafion/Tyr/EGR–AuNPs–Ch/GCE gave roughly symmetric anodic and cathodic peaks at relative slow scan rates. When the scan rate increased, the redox potentials (E_{pa} and E_{pc}) of Tyr hardly shift. Meanwhile, the redox peak current increased linearly (inset, Fig. 4): I_{pa} = -3.7×10^{-1}–1.4×10^{-1} v, r = 0.9996; I_{pc}= 9.5×10^{-1} +1.2×10^{1} v, r= 0.9996. The high electroactive area of EGR–AuNPs–Ch induces high capacitance [11] and, high background currents varying proportionally with the scan rate. This indicated that the electron transfer process for Tyr at the Nafion/Tyr/EGR–AuNPs–Ch/GCE was a surface–confined mechanism in the above–mentioned potential scope, manifesting the characteristics of thin–layer surface–controlled electrochemical process.

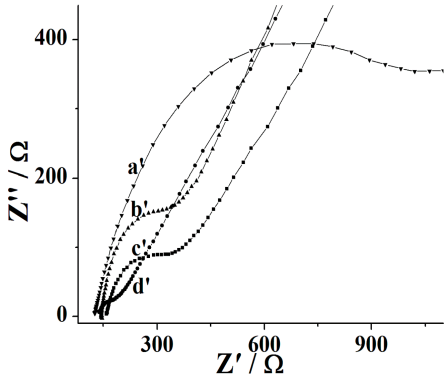

Fig. 3 EIS plots for the bare GCE (a'), the AuNPs–Ch/GCE (b'), the Nafion/Tyr/EGR–AuNPs–Ch/GCE (c') and the EGR–AuNPs–Ch/GCE (d') in a solution of 5 mM $[Fe(CN)_6]^{3-/4-}$+ 0.1 M KCl as the supporting electrolyte. The frequencies swept from 10^5 to 10^{-2} Hz.

The anodic and cathodic peak potentials were linearly dependent on the logarithm of the scan rates (n) with slopes of $-2.3RT/anF$ and $2.3RT/(1-a)nF$, respectively. Hence, the charge–transfer coefficient a was calculated as 0.47. Heterogeneous electron transfer rate constant (k_s) was further estimated according to the following equation [51]:

$$log\ k_s = a\log(1-a) + (1-a)\ log a - log\ (RT/nFv)$$

$$-(1-a)\ aF\Delta E_p/(2.3RT) \qquad (1)$$

Where a is charge transfer coefficient. n is the number of electron transfer. R, T and F symbols have their conventional meanings. ΔE_p is the peak to peak potential separation.

Preprints (www.preprints.org) | NOT PEER-REVIEWED | Posted: 28 April 2017 doi:10.20944/preprints201704.0188.v1

Peer-reviewed version available at Molecules 2017, 22, 1047; doi:10.3390/molecules22071047

The result was 0.66 s^{-1}, which was higher than that 0.032s^{-1} of the Tyr–AuNPs/ boron-doped diamond (BDD) [52] and 0.030 s^{-1} of the Tyr/AgE [23]. Thus, Nafion/Tyr/EGR–AuNPs–Ch/GCE can provide a favorable microenvironment for Tyr to undergo a facile electron transfer reaction due to the structure of EGR–AuNPs–Ch is to the benefit of effective immobilization of enzyme, protein and other bioactive substances. EGR greatly increased the specific surface area and shorten the distance between the active centre of Tyr and the electrode surface. Furthermore, interlayers offered more binding sites for the immobilization of Tyr.

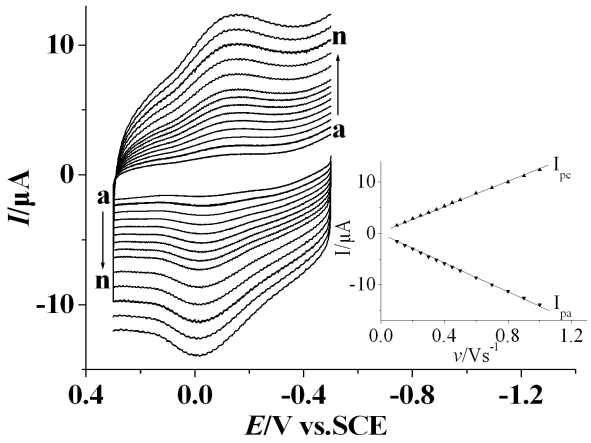

Fig. 4 CVs of the Nafion/Tyr/EGR–AuNPs–Ch/GCE in N_2–saturated PBS with different scan rates (from a to n: 100, 150, 200, 250, 300, 350, 400, 450, 500, 600, 700, 800, 900, 1000 mV/s). Inset: the relationship between cathodic and anodic peak current with scan rate *v*.

3.3. Amperometric response towards CA

The possible mechanism of electrocatalytic reduction of CA at Tyr−based enzyme electrode could be expressed as follows (Scheme 2).

$$\text{catechol} + \text{tyrosinase } (O_2) \rightarrow o\text{–quinone} + H_2O \qquad (2)$$

But, *o*–quinone is extremely unstable, an accompanying reaction was following [44]:

$$o\text{–quinone} + 2H^+ + 2e^- \rightarrow \text{catechol} \qquad (3)$$

Similar structure compounds such as gallic acid, caffeic acid, p–coumaric acid and ferulic acid were also determined by the Nafion/Tyr/EGR–AuNPs–Ch/GCE. As derivative of CA, caffeic acid current response towards the same concentration was only one fifth to one third of CA. The quite similar structure of caffeic acid made it easily catalyze by Tyr. The carboxyl group and double bond contributed to the current drop. Gallic acid showed slight current change. The third hydroxyl severely hindered the catalytic process of Tyr due to steric effect. There were no remarkable current changed of p–coumaric

Preprints (www.preprints.org) | NOT PEER-REVIEWED | Posted: 28 April 2017 doi:10.20944/preprints201704.0188.v1

Peer-reviewed version available at Molecules 2017, 22, 1047; doi:10.3390/molecules22071047

acid and ferulic acid. Monophenols are hydroxylated to a variety of to diphenols and then catalyzed by Tyr subsequent oxidation to quinines [53]. EGR can interact with the double bond of p–coumaric acid and ferulic acid by the π–π attraction, which block the monophenols hydroxylation, resulting the difficult of Tyr catalysis. The above results confirmed the mechanism of electrocatalytic reduction of CA at Nafion/Tyr/EGR–AuNPs–Ch/GCE.

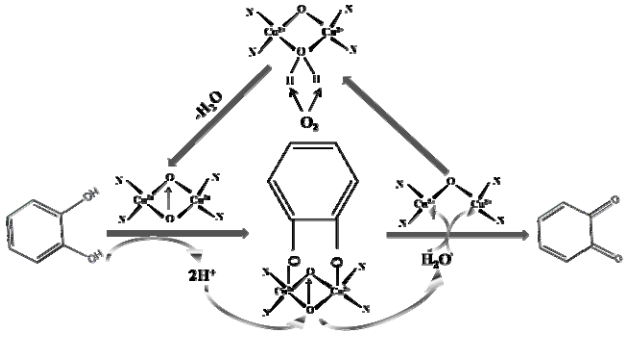

Scheme 2. Schematics of the possible mechanism of catalytic oxidization of Tyr towards catechol at the Nafion/Tyr/EGR–AuNPs–Ch/GCE.

Chronoamperometry was also used for the investigation of electrocatalytic of CA at the Nafion/Tyr/EGR–AuNPs–Ch/GCE. Effect of applied potential was investigated at different potentials ranging from 0.10 V to –0.30 V. At the applied potentials from 0.10 V to –0.10 V, the current increased and reached a peak plateau. From –0.10 V to –0.30 V, the response of the electrode gradually decreased. Moreover, the baseline current of the signal became unstable above –0.10 V. As a result, –0.10 V was finally chosen as the applied potential throughout all the amperometric measurements.

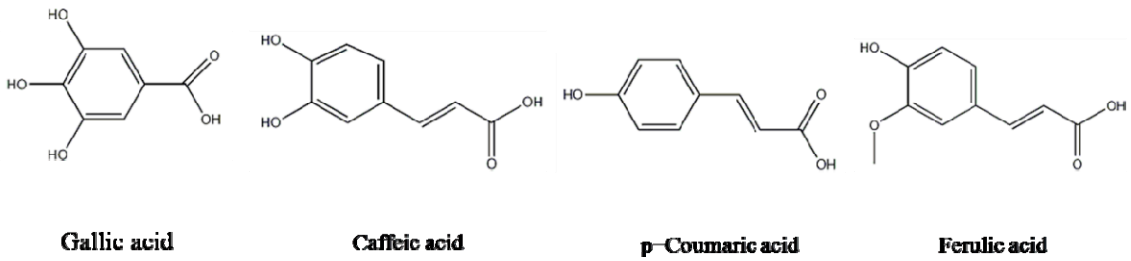

Scheme 3. The structure of gallic acid, caffeic acid, p–coumaric acid and ferulic acid.

Fig. 5 shows the amperometric current–time curves were performed to study the performance of the fabricated electrodes on successive addition of CA. When CA was added into the stirring 0.1 M, pH 7.0 PBS, a quick response to the substrate happened. The proposed Nafion/Tyr/EGR–AuNPs–Ch/GCE (d") got the best amperometric response as expected. Comparing with the bare GCE (a"), the AuNPs–Ch/GCE (b") and the EGR–AuNPs–Ch/GCE (c") upon the addition of 5 μM of CA into a

Preprints (www.preprints.org) | NOT PEER-REVIEWED | Posted: 28 April 2017 doi:10.20944/preprints201704.0188.v1

Peer-reviewed version available at Molecules 2017, 22, 1047; doi:10.3390/molecules22071047

continuous stirring PBS at –0.10 V, the current response of the Nafion/Tyr/EGR–AuNPs–Ch/GCE increase dramatically.

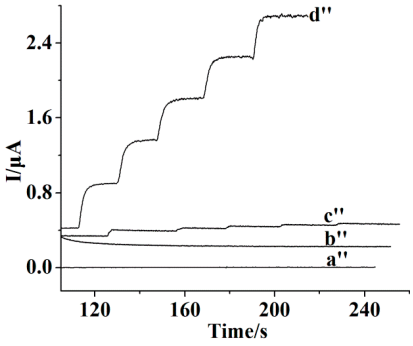

Fig. 5 Amperometric responses of the bare GCE (a''), the AuNPs–Ch/GCE (b''), the EGR–AuNPs–Ch/GCE(c'') and Nafion/Tyr/EGR–AuNPs–Ch/GCE (d'') at –0.10 V (*vs.* SCE) upon successive addition of the same concentration of CA.

Fig.6 illustrated a typical current–time curve of the sensor based on the Nafion/Tyr/EGR–AuNPs–Ch/GCE upon the addition of an aliquot concentration of CA into a continuous stirring of 0.1 M, pH 7.0 PBS at optimal condition. Even with 0.25 μM of CA, as shown in Fig. 6 insert A, obvious amperometric responses were shown. The 95% of steady–state current can be obtained at 2–3 s, revealing the faster response of the sensor than that of previously reported CA sensors [7, 54]. The current response increased along with CA concentration. The calibration curve at the biosensor showed linearity from 0.2 to 270 μM (Fig. 6 insert B). The linear regression equation was got as I_{ss} (μA) = 9.11×10^{-2} C (μM) + 5.13×10^{-1} (r =0.9962) with a detection limit of 0.1 μM (S/N=3). The biosensor had a much better catalytical response towards CA than that of the agarose–guar gum entrapped Tyr [10] and PANI–polyphenol oxidase (PPO) film[14].

According to Michaelis−Menten kinetic mechanism, the apparent Michaelis–Menten constant K_M^{app} can be obtained from the electrochemical version of the Lineweaver–Burk equation [55, 56]

$$1/I_{ss} = 1/I_{max} + K_M^{app}/(I_{max}C) \qquad (4)$$

Here I_{ss} is the diffusion limiting current after the addition of the substrate. C is the bulk concentration of the substrate, and I_{max} is the maximum current measured under the saturate substrate conditions. The value of K_M^{app} and I_{max} can be obtained by the slope and the intercept of the plot of the reciprocals of the steady–state current versus catechol concentration. The apparent Michaelis−Menten constant K_M^{app} value was calculated to be 109 μM, which was much lower than some previous reports [14, 57]. The K_M^{app} value reflects the affinity of the enzyme for the substrate: the smaller the K_M^{app} value,

Preprints (www.preprints.org) | NOT PEER-REVIEWED | Posted: 28 April 2017 doi:10.20944/preprints201704.0188.v1

Peer-reviewed version available at Molecules 2017, 22, 1047; doi:10.3390/molecules22071047

the greater the affinity [58]. So the lower value of K_M^{app} indicates that the immobilized Tyr exhibited stronger affinity to catechol than that of the free Tyr [59]. And, Tyr can retain higher activity in the Nafion/Tyr/EGR–AuNPs–Ch/GCE. This methodology provides graphene–nanomaterial composite films with low cost, no chemical use, massively parallel, and controllability of nanomaterial composition.

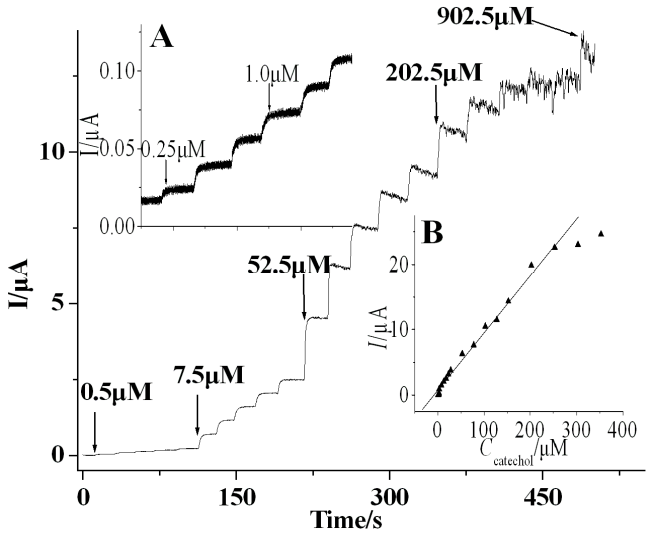

Fig. 6 Amperometric responses of the Nafion/Tyr/EGR–AuNPs–Ch/GCE at –0.10 V (*vs.* SCE) upon successive addition of 0.5 μM, 7.5 μM, 52.5 μM, 202.5 μM and 902.5 μM CA in PBS. Inset: (A) Amperometric responses of the Nafion/Tyr/EGR–AuNPs–Ch/GCE at 0.20 V (*vs.* SCE) upon successive addition of 0.25 μM and 1.0 μM CA in PBS; (B) Plot of peak current *vs*. CA concentration.

3.4. Repeatability and stability of CA biosensor

The stability and repeatability of the biosensor were studied. The relative standard deviation (RSD) was 2.4% for eight successive measurements of 10 μM CA in PBS, showed the proposed biosensor possessed a good repeatability. The cyclic voltammetric responses of the modified biosensor in PBS containing 10 μM CA showed no obvious change after 25 cycles, and then it decreased slowly with the increase of the cycle, indicating that the biosensor was stable. The storage stability the biosensor was further investigated. The peak currents of the Nafion/Tyr/EGR–AuNPs–Ch/GCE was measured using the same electrode and it retained above 95% of its initial response stored at 4 °C after 3 weeks. These results displayed that the biosensor based on the Nafion/Tyr/EGR–AuNPs–Ch/GCE had a good stability.

4. Conclusions

In the present work, GR was *in situ* prepared on choline functionalized gold nanoparticals (AuNPs–Ch) modified GCE successfully. With the EGR–AuNPs–Ch/GCE as the platform, CA

biosensor exhibited a variety of good electrochemical characteristics, including low detection limit, high catalytic ability, wide linearity and a larger electron transfer rate constant of 0.66 s^{-1}. These advantages should be attributed to the following: (1) AuNPs–Ch can be efficiently immobilized on the bare GCE, and interlayer EGR provide more attach site for Tyr immobilization; (2) π–π electron transfer between AuNPs–Ch and EGR, plays an important role in facilitating the electron transfer between Tyr and the electrode surface; (3) Synergistic effects of AuNPs–Ch and EGR exhibited the signal amplification of nanosize materials.

Acknowledgements

The authors gratefully acknowledge the financial support of this project by the National Science Foundation of China (No. 21445004、21545014、21643014、21275116), the Scientific Research Plan Projects of the Education Department of Shaanxi Province, China (No. 14JS095), Xi'an Science and Technology Plan Project (No. CXY1443WL27) , Dr. Startup funds from Xi'an University(No. 06005017) and the development transformation of key disciplines in Shaanxi provincial-analytical chemistry(09009001).

References

[1] A. Alessandra, S. Matteo, D. Stephan, M. Saverio, Nanofibrous membrane based tyrosinase-biosensor for the detection of phenolic compounds, Anal. Chim. Acta, 659 (2010) 133–136.

[2] W. Du, F.Q. Zhao, B.Z. Zeng, Novel multiwalled carbon nanotubes–polyaniline composite film coated platinum wire for headspace solid-phase microextraction and gaschromatographic determination of phenolic compounds, J. Chrom. A, 1216 (2009) 3751–3757.

[3] M. Guix, B. Pérez–López, M. Sahin, M. Roldán, A. Ambrosi, A. Merkoçi, Structural characterization by confocal laser scanning microscopy and electrochemical study of multi walled carbon nanotube tyrosinase matrix for phenol detection. Analyst, 135 (2010) 1918–1925.

[4] S.F. Wang, Y.M. Tan, D.M. Zhao, G.D. Liu, Amperometric tyrosinase biosensor based on Fe_3O_4 nanoparticles-chitosan nanocomposite. Biosens. Bioelectron., 23 (2008) 1781–1787.

[5] L.M. Lu, L. Zhang, X.B. Zhang, S.Y. Huan, G.L. Shen, R.Q. Yu, A novel tyrosinase biosensor based on hydroxyapatite–chitosan nanocomposite for the detection of phenolic compounds, Anal. Chim. Acta, 665 (2010) 146–151.

[6] E. Burestedt, A. Narvaez, T. Ruzgas, L. Gorton, J. Emnéus, E. Domínguez, G. Marko–Varga, Rate limiting steps of tyrosinase–modified electrode for detection of catechol, Anal. Chem., 68 (1996) 1605–1611.

[7] J. Zhang, J.P. Lei, Y.Y. Liu, J.W. Zhao, H.X. Ju, Highly sensitive amperometric biosensors for phenols based on polyaniline–ionic liquid–carbon nanofiber composite, Biosens. Bioelectron., 24 (2009) 1858–1863.

[8] S. Alwarappan, C. Liu, A. Kumar, C.Z. Li, Enzyme–doped graphene nanosheets for enhanced glucose biosensing, J. Phys. Chem. C, 114 (2010) 12920–12924.

[9] B. Pérez–López, A. Merkoçi, Magnetic nanoparticles modified with carbon nanotubes for electrocatalytic magnetoswitchable biosensing applications, Adv. Funct. Mater., 21 (2011) 255–260.

[10] S. Tembe, S. Inamdar, S. Haram, M. Karve, S.F. D'Souza, Electrochemical biosensor for catechol using agarose–guar gumentrapped tyrosinase. J. Biotech., 128 (2007) 80–85.

[11] B. Reuillard, A.L. Goff, C. Agnès, A. Zebda, M. Holzinger, S. Cosnier, Direct electron transfer between tyrosinase and multi–walled carbon nanotubes for bioelectrocatalytic oxygen reduction, Electrochem. Commun., 20 (2012) 19–22.

[12] E.J. Jang, K.J. Son, B. Kim, W.G. Koh, Phenol biosensor based on hydrogel microarrays entrapping tyrosinase and quantum dots, Analyst, 135 (2010) 2871–2878.

[13] L.J. Yang, H.Y. Xiong, X.H. Zhang, S.F. Wang. A novel tyrosinase biosensor based on

chitosan-carbon-coated nickel nanocomposite film, Bioelectrochemistry, 84 (2012) 44–48.

[14] Y.Y. Tan, J.Q. Kan, S.Q. Li, Amperometric biosensor for catechol using electrochemical template process, Sens. Actuators B: Chem., 152 (2011) 285–288.

[15] L.M. Lu, L. Zhang, X.B. Zhang, S.Y. Huan, G.L. Shen, R.Q. Yu, A novel tyrosinase biosensor based on hydroxyapatite–chitosan nanocomposite for the detection of phenolic compounds, Anal. Chim. Acta, 665 (2010) 146–151.

[16] J.W. Zhao, D.H. Wu, J.F. Zhi, A novel tyrosinase biosensor based on the nanocrystalline diamond electrode for detection of phenolic compounds, Bioelectrochemistry, 75 (2009) 44–49.

[17] M. ElKaoutit, I. Naranjo–Rodriguez, K.R. Temsamani, M. Domínguez, J.L. Hidalgo–Hidalgo de Cisneros, A comparison of three amperometric phenoloxidase–sonogel–carbon based biosensor for determination of polyphenols in beers, Talanta, 75 (2008) 1348–1355.

[18] H.S. Yin, Y.L. Zhou, J. Xu, S.Y. Ai, L. Cui, L.S. Zhu, Amperometric biosensor based on tyrosinase film and its applicationto determine bisphenol A, Anal. Chim. Acta, 659 (2010) 144–150.

[19] B. Reuillard, A.L. Goff, C. Agnès, A. Zebda, M. Holzinger, S. Cosnier, Direct electron transfer between tyrosinase and multi–walled carbon nanotubes for bioelectrocatalytic oxygen reduction, Electrochem. Commun., 20 (2012) 19–22.

[20] H. Faridnouri, H. Ghourchian, S. Hashemnia, Direct electron transfer enhancement of covalently bound tyrosinase to glassy carbon via Woodward's reagent K, Bioelectrochemistry, 82 (2011) 1–9.

[21] A. Mohammadi, A.B. Moghaddam, R. Dinarvand, S. Rezaei–Zarchi, Direct electron transfer of polyphenol oxidase on carbon nanotube surfaces: application in biosensing, Int. J. Electrochem. Sci., 4 (2009) 895–905.

[22] B.C. Janegitz, R.A. Medeiros, R.C. Rocha-Filho, O. Fatibello–Filho, Direct electrochemistry of tyrosinase and biosensing for phenol based on gold nanoparticles electrodeposited on a boron doped dimond electrode, Diam. Relat. Mater., 25 (2012) 128–133.

[23] A.B. Moghaddam, M.R. Ganjali, A.A. Saboury, A.A. Moosavi–Movahedi, Parviz Norouzi, Electrodeposition of nickel oxide nanoparticles on glassy carbon surfaces: application to the direct electron transfer of tyrosinase, J. Appl. Electrochem., 38 (2008) 1233–1239.

[24] S.F. Hou, M.L. Kasner, S.J. Su, K. Patel, R. Cuellari, Highly sensitive and selective dopamine biosensor fabricated with silanized graphene, J. Phys. Chem. C, 114 (2010) 14915–14921.

[25] J. Luo, S.S. Jiang, H.Y. Zhang, J.Q. Jiang, X.Y. Liu, A novel non–enzymatic glucose sensor based on Cu nanoparticle modified graphene sheets electrode, Anal. Chim. Acta, 709 (2012) 47–53.

[26] M. Zhou, Y.M. Zhai, S.J. Dong, Electrochemical sensing and biosensing platform based on chemically reduced graphene oxide, Anal. Chem., 81 (2009) 5603–5613.

[27] L.H. Tang, Y. Wang, Y.M. Li, H.B. Feng, J. Lu, J.H. Li. Preparation, structure and electrochemical

properties of graphene modified electrode, Adv. Funct. Mater., 19 (2009) 2782–2789.

[28] D. Chen, L.H. Tang, J.H. Li, Graphene-based materials in electrochemistry, Chem. Soc. Rev., 39 (2010) 3157–3180.

[29] J. Bai, Y.J. Lai, D.W. Jiang, Y.B. Zeng, Y.Z. Xian, F. Xiao, N.D. Zhang, J. Hou, L.T. Jin, Ultrasensitive electrochemical immunoassay based on graphene oxide–Ag composites for rapid determination of clenbuterol, Analyst, 137 (2012) 4349–4355.

[30] J.B. Zheng, Y.P. He, Q.L. Sheng, H.F. Zhang, DNA as a linker for biocatalytic deposition of Au nanoparticles on graphene and its application in glucose detection, J. Mater. Chem., 21 (2011) 12873–12879.

[31] Y.P. He, Q.L. Sheng, J.B. Zheng, M.Z. Wang, B. Liu, Magnetite–graphene for the direct electrochemistry of hemoglobin and its biosensing application, Electrochim. Acta, 56 (2011) 2471–2476.

[32] C.B. Liu, K. Wang, S.L. Luo, Y.H. Tang, L.Y. Chen, Direct electrodeposition of graphene enabling the one−step synthesis of graphene−metal nanocomposite films, Small, **7** (2011) 1203–1206.

[33] H.L. Guo, X.F. Wang, Q.Y. Qian, F.B. Wang, X.H. Xia, A green approach to the synthesis of graphene nanosheets. ACS nano, 3 (2009) 2653–2659.

[34] B. Unnikrishnan, S. Palanisamy, S.M. Chen, A simple electrochemical approach to fabricate a glucose biosensor based on graphene–glucose oxidase biocomposite, Biosens. Bioelectron., 39 (2013) 70–75.

[35] Q.L. Sheng, Y.P. He, D.W. Zhang, J.B. Zheng, Ultrasonic–electrodeposition of flower–like graphene nanosheets in ionic liquid and its sensing for ascorbic acid, J. Chin. Chem. Soc., (2013) 60(2013) 199–203.

[36] Y.P. He, J.B. Zheng, S.Y. Dong, Ultrasonic–electrodeposition of hierarchical flower–like cobalt on petalage-like graphene hybrid microstructures for hydrazine sensing. Analyst, 137 (2012) 4841–4848.

[37] Y.P. He, Jianbin Zheng, One–pot ultrasonic–electrodeposition of copper–graphene nanoflowers in Ethaline for glucose sensing, Anal. Methods, 5 (2013) 767–772.

[38] C.S. Shan, H.F. Yang, D.X. Han, Q.X. Zhang, A. Ivaska, L. Niu, Water–soluble graphene covalently functionalized by biocompatible poly–L–lysine, Langmuir, 25 (2009) 12030–12033.

[39] L.P. Jiang, R. Yuan, Y.Q. Chai, Y.L. Yuan, L.J. Bai, Y. Wang, Aptamer–based highly sensitive electrochemical detection of thrombin via the amplification of graphene, Analyst, 137 (2012) 2415–2420.

[40] D. Du, Z.X. Zou, Y.S. Shin, J. Wang, H. Wu, M.H. Engelhard, J. Liu, I.A. Aksay, Y.H. Lin, Sensitive immunosensor for cancer biomarker based on dual signal amplification strategy of

graphene sheets and multienzyme functionalized carbon nanospheres, Anal. Chem., 82 (2010) 2989–2995.

[41] K. Saha, S.S. Agasti, C. Kim, X.N. Li, V.M. Rotello, Gold nanoparticles in chemical and biological sensing, Chem. Rev., 112 (2012) 2739–2779.

[42] P. Kannan, S.A. John, Determination of nanomolar uric and ascorbic acids using enlarged gold nanoparticles modified electrode, Anal. Biochem., 386 (2009) 65–72.

[43] K.L. Adams, B.K. Jena, S.J. Percival, B. Zhang, Highly sensitive detection of exocytotic dopamine release using a gold–nanoparticle–network microelectrode, Anal. Chem., 83 (2011) 920–927.

[44] W. Song, D.W. Li, Y.T. Li, Y. Li,Y.T. Long, Disposable biosensor based on graphene oxide conjugated with tyrosinase assembled gold nanoparticles, Biosens. Bioelectron., 26 (2011) 3181–3186.

[45] Y. Zheng, X.Q. Lin, Modified electrode based on immobilizing horseradish peroxidase on nano–gold with choline covalently modified glassy carbon electrode as a base, Chin. J. Anal. Chem., 36 (2008) 604–608.

[46] Y.X. Li, X.Q. Lin, C.M. Jiang, Fabrication of a nanobiocomposite film containing heme proteins and carbon nanotubes on a choline modified glassy carbon electrode: direct electrochemistry and electrochemical catalysis, Electroanalysis, 18 (2006) 2085–2091.

[47] W.S. Hummers, R.E. Offeman, Preparation of graphitic oxide, J. Am. Chem. Soc. 80 (1958) 1339.

[48] P. Wang, Y.X. Li, X. Huang, L. Wang, Fabrication of layer–by–layer modified multilayer films containing choline and gold nanoparticles and its sensing application for electrochemical determination of dopamine and uric acid, Talanta, 73 (2007) 431–448.

[49] T. Gan, S.S. Hu, Electrochemical sensors based on graphene materials, Microchim. Acta, 175 (2011) 1–19.

[50] S. Shleev, J. Tkac, A. Christenson, T. Ruzgas, A.I. Yaropolov, J.W. Whittaker, L. Gorton, Amperometric biosensors based on recombinant laccases for phenols determination, Biosens. Bioelectron., 20 (2005) 2517–2554.

[51] E. Laviron, General expression of the linear potential sweep voltammogram in the case of diffusionless electrochemical systems, J. Electroanal. Chem., 101 (1979) 19–28.

[52] B.X. Ye, X.Y. Zhou, Direct electrochemical redox of tyrosinase at silver electrodes, Talanta, 44 (1997) 831–836.

[53] D.Y. Xu, Y. Yang, Z. Yang, Activity and stability of cross–linked tyrosinase aggregates in aqueous and nonaqueous media, J. Biotech., 152 (2011) 30–36.

[54] L.J. Yang, H.Y. Xiong, X.H. Zhang, S.F. Wang, A novel tyrosinase biosensor based on chitosan–carbon–coated nickel nanocomposite film, Bioelectrochemistry, 84 (2012) 44–48.

[55] R. A. Kamin, G. S. Wilson, Rotating ring-disk enzyme electrode for biocatalysis kinetic studies and characterization of the immobilized enzyme layer, Anal. Chem., 52 (1980) 1198–1205.

[56] F. R. Shu, G. S. Wilson, Rotating ring-disk enzyme electrode for surface catalysis study, Anal. Chem., 48 (1976) 1679–1686.

[57] M. S. López, E. pez–Cabarcos, B. López–Ruiz, Influence of the host matrix of the enzyme in the performance of amperometric biosensors, Sens. Actuators B: Chem., 171–172(2012) 387–397.

[58] P. Pandey, S.P. Singh, S.K. Arya, V. Gupta, M. Datta, S. Singh, B.D. Malhotra, Application of thiolated gold nanoparticles for the enhancement of glucose oxidase activity. Langmuir, 23 (2007) 3333–3337.

[59] S. Kiralp, L. Toppare, Polyphenol content in selected Turkish wines, an alternative method of detection of phenolics, Process Biochem., 41 (2006) 236–239.